Hindawi
International Journal of RF and Microwave Computer-Aided Engineering
Volume 2024, Article ID 5076232, 12 pages
https://doi.org/10.1155/2024/5076232

Research Article

A Dual-Band Low SAR Microstrip Patch Antenna with Jean Substrate for WBAN Applications

Wanwisa Thaiwirot,[1] **Yotrawee Hengroemyat**,[1] **Thamonwan Kaewthai**,[1] **Prayoot Akkaraekthalin**,[1] **and Suramate Chalermwisutkul**[2]

[1]*Department of Electrical and Computer Engineering, King Mongkut's University of Technology North Bangkok (KMUTNB), Bangkok 10800, Thailand*
[2]*The Sirindhorn International Thai-German Graduate School of Engineering (TGGS), King Mongkut's University of Technology North Bangkok (KMUTNB), Bangkok 10800, Thailand*

Correspondence should be addressed to Wanwisa Thaiwirot; wanwisa.t@eng.kmutnb.ac.th

Received 2 November 2023; Revised 5 March 2024; Accepted 7 March 2024; Published 23 March 2024

Academic Editor: Alessandro Di Carlofelice

This paper presents a low-profile dual-band microstrip patch antenna operated at the 2.45/5.8 GHz ISM bands, targeting wireless body area network (WBAN) applications. The proposed antenna is fabricated on a jean substrate measuring $74 \times 82\,mm^2$. The four corners of the conventional rectangular patch are cut to activate an additional operating frequency and to enhance the radiation pattern. The circular slot is added to the radiating patch to fine-tune the desired frequencies. The measured impedance bandwidth of the proposed antenna at 2.45 GHz and 5.8 GHz bands is 3.68% (2.40 GHz–2.49 GHz) and 3.81% (5.67 GHz–5.89 GHz), respectively. The measured maximum gains are 3.08 dBi at 2.45 GHz and 2.15 dBi at 5.8 GHz. Moreover, the antenna's performance when placed on flat and rounded body surfaces is also investigated. The proposed antenna achieves stable radiation pattern and low specific absorption rate (SAR) value with low complexity in design. The results indicate that the proposed antenna can be a promising candidate for WBAN applications.

1. Introduction

Wireless body area network (WBAN) has been receiving significant attention in recent years due to their versatile applications in fields such as healthcare, sports, fitness, military, and entertainment [1]. As a result, the need for stable wireless connections and high data rates has become more important. The antennas are an important role in meeting these requirements. The design of antennas on flexible materials, which can be used both on curved surfaces or on human body, is a challenge for a researcher. The merits of flexible antenna are the ability to bend on the different surfaces, unobtrusive for users, lightweight, and low cost, making them suitable for WBAN [2, 3]. In practice, the wearable antennas can be integrated with clothing or wearable devices, which are in close proximity to human body. It is well known that the antenna's performance is degraded when the antenna is in proximity to the human body. Therefore, the effects of the human body on antenna's performance should be considered. In addition, the radiation toward human body from wearable antennas should be as small as possible for the safety of human tissue. The Federal Communication Commission (FCC) introduced a specific absorption rate (SAR) limit for wearable devices to ensure acceptable radiation level in human body. The FCC SAR limit is 1.6 W/kg over 1 g of actual tissue, while the Council of the European Union SAR limit is 2.0 W/kg over 10 g of actual tissue [4]. Several flexible and wearable antennas have been designed for WBAN applications such as planar monopole antenna [5], planar dipole antenna [6], slot antenna [7], fractal antenna [8], and microstrip patch antenna [9]. The multiband fractal antenna with dendrite structure based on

monopole antenna was presented in [10]. The antenna was designed on polymide substrate. Although the antenna can provide good performance, the SAR value was not mentioned in this paper. As is well known, the monopole, dipole, and slot antennas have backward radiations, which yield the SAR value exceeding the standard. Hence, the reflector should be placed behind these antennas in order to reduce the backward radiations toward human body [11–13]. In [14], the dual-band T-shaped monopole antenna was proposed. The 2×2 EBG structure was placed behind the antenna to reduce the interference from human body and to reduce the SAR. The EBG structure reduced the SAR value by 77.1% and 91.7% at 2.4 GHz and 5.2 GHz, respectively. Although the proposed antenna with reflector can eliminate the impact of the human body on antenna performance and decrease the SAR, they cannot be fabricated as a low-profile structure. Therefore, flexible microstrip patch antennas operating within the 2.4 GHz (2.40 GHz–2.48 GHz) and 5.8 GHz (2.725 GHz–5.875 GHz) for industrial, scientific, and medical (ISM) bands are focused in this paper. It is well known that the microstrip patch antenna has unidirectional radiation pattern. Thus, it is safe when used on human body. Microstrip patch antennas with different flexible substrates, such as epoxy, Teflon, polyethylene, PI, RT Duroid, and PDMS were proposed in [15]. It is found that the textile materials show a low dielectric constant as compared with polymer-based materials which make them to have lower surface wave losses [16]. Several textile microstrip patch antennas were presented [17–25]. For example, the design of textile conventional microstrip patch antenna to operate at 2.45 GHz was presented in [17]. The authors used jean as substrate, which has a dielectric constant of 1.7. The SAR level of this textile microstrip patch antenna was found to be 1.14 W/kg and 0.742 W/kg for 1 g and 10 g of tissue, respectively. In [18], the textile rectangular patch antenna constructed using polyester as substrate was presented. The defected ground plane (DGS) technique was used on the ground layer to increase antenna's performance. The antenna can operate at 2.4 GHz in the ISM band with good radiation characteristics. However, the SAR value of the antenna with the DGS ground plane exceeded 1.6 W/kg for 1 g of tissue. Thus, the microstrip patch antenna with a full ground plane provides low SAR values. Moreover, in order to add one or more resonant frequencies for various wireless frequency bands, the multiple slots were etched into the conventional radiating patch to operate at 5.8, 6.2, and 8.4 GHz [19]. However, etching the slots on the radiating patch to create a new resonant frequency causes an unstable radiation pattern. In [20], an inverted U-shaped slot was added to the conventional patch to generate a second resonant frequency. The partial ground plane was used to increase the bandwidth and gain. However, the use of the partial ground plane provides relatively unsatisfactory SAR value, and the rigid substrate may make it obtrusive for users. The dual-band circular patch antenna using annual slots was proposed in [21]. However, the combination between rigid and textile substrates and the use of coaxial feeding technique make wearing uncomfortable. In [22], a wearable all-textile multiband circular patch antenna using slot loading techniques was proposed. The antenna has good properties, especially in terms of wearing comfort, but the antenna gain is relatively low in all bands.

This paper presents the design and analysis of the dual-band textile microstrip antenna for WBAN applications. The proposed microstrip antenna is made of jean as the substrate and copper sheet as the radiating patch and ground plane. Initially, the antenna is designed to operate at 2.45 GHz. Then, four corners of rectangular patch are cut to excite the additional resonant frequency at 5.8 GHz. The circular slot is loaded on the patch to fine-tune the desired operating frequency bands. The proposed antenna not only can operate in ISM bands at 2.45 GHz and 5.8 GHz but also achieves low profile, lightweight, and bendable. Furthermore, the antenna performance under different bending conditions in free space as well as when it is placed on human body is presented and discussed. The SAR limits are also investigated to confirm that the proposed antenna is harmless to human body. The simulated and measured results indicate that the proposed antenna provides good performance within operating frequency bands. The design and analysis of the proposed antenna by using CST software are discussed below.

2. Antenna Structure and Design

The basic configuration of the proposed antenna consists of radiating patch, microstrip line feed, and ground plane as shown in Figure 1. The proposed antenna is designed on jean substrate with a relative permittivity of 1.7, a loss tangent of 0.02, and a thickness of 1 mm [26]. The jean substrate is selected because of the low dielectric constant, low cost, flexibility, and convenient availability. The copper sheet with the thickness of 0.1 mm is attached to the jean substrate to form the radiator and ground plane.

In the antenna designing process, the rectangular patch which corresponds to the resonant frequency at 2.45 GHz is designed in the first stage as shown in Figure 1(a). The width (W_p) and length (L_p) of the rectangular patch are evaluated using Equations (1) and (2) according to [27],

$$W_p = \frac{c_0}{2f_r}\sqrt{\frac{2}{\varepsilon_r + 1}}, \tag{1}$$

where c_0 is the speed of light (3×10^8 m/s). ε_r is the relative permittivity of the substrate. f_r is the resonant frequency which is defined as 2.45 GHz. The length of patch is calculated by

$$L_p = \frac{c_0}{2f_r\sqrt{\varepsilon_{\text{eff}}}} - 2\Delta L_p. \tag{2}$$

The ΔL_p is the effective length of the patch due to fringing effect. The ε_{eff} is effective relative permittivity which can be calculated in

$$\varepsilon_{\text{eff}} = \frac{\varepsilon_r + 1}{2} + \frac{\varepsilon_r + 1}{2}\left(1 + 12\frac{h}{W_p}\right)^{-1/2}. \tag{3}$$

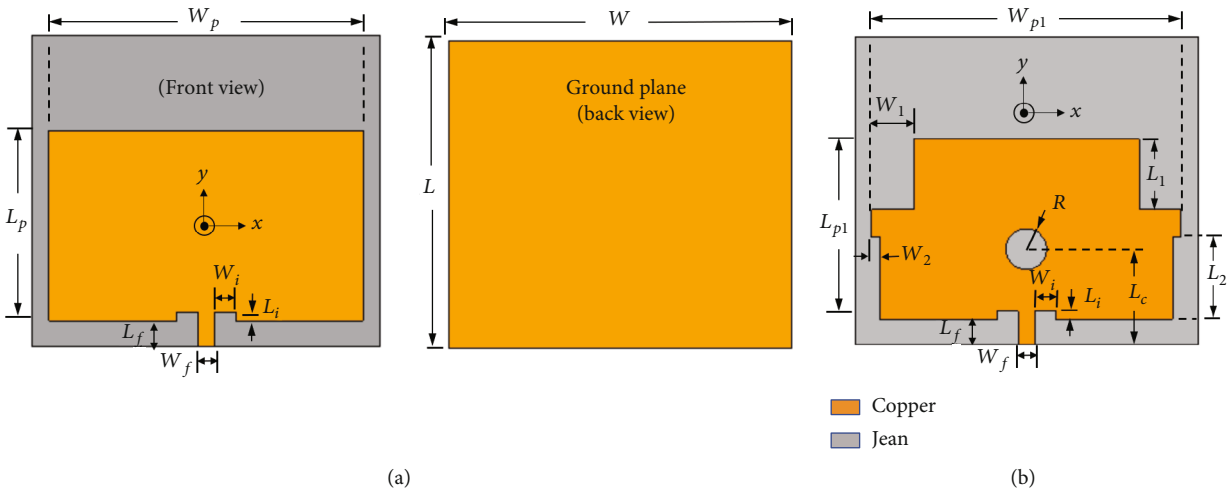

Figure 1: Configuration of the textile microstrip patch antenna: (a) conventional inset-fed rectangular microstrip patch antenna and (b) proposed antenna.

Table 1: Parameter values of the proposed antenna.

Parameters	Values (mm)	Parameters	Values (mm)
W_{p1}	74	W_1	10
L_{p1}	43	L_1	17
L_f	6	W_2	2
W_f	4	L_2	20
L_i	2	W_i	5
W	82	L_c	22
L	74	R	5

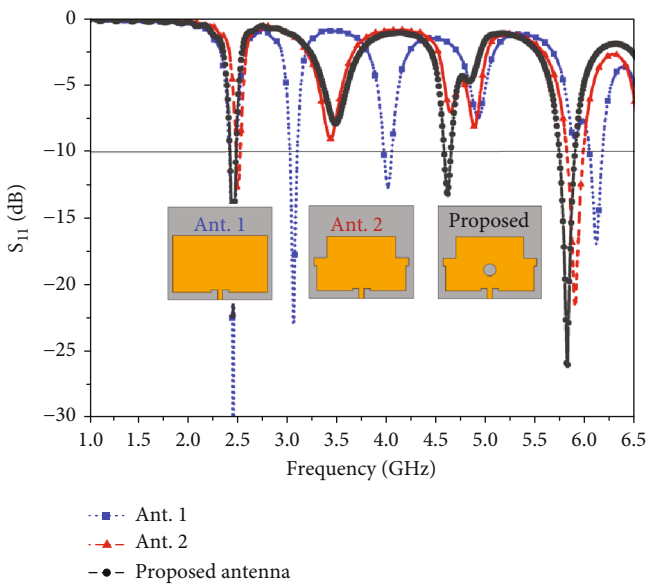

Figure 2: The simulated S_{11} for the three antenna design stages.

h is the substrate height. The change in the length of patch due to its fringing effect is given by

$$\Delta L_p = 0.412h\frac{(\varepsilon_{\text{eff}}+0.300)}{(\varepsilon_{\text{eff}}+0.258)}\frac{((W_p/h)+0.264)}{((W_p/h)+0.8)}. \quad (4)$$

The width and length of rectangular patch are calculated using Equations (1) and (2) to be $W_p = 53$ mm and $L_p = 46$ mm, respectively. The width and length of the 50 ohm microstrip feed line are $W_f = 4$ mm and $L_f = 6$, respectively. Moreover, the inset feed technique is used to improve impedance matching of the antenna by etching the thin slot along the bottom edge of radiating patch. The width and length of the inset are $W_i = 5$ mm and $L_i = 1$ mm, respectively. From the study of parameters, the length (L_p) of rectangular patch affects the resonant frequency of the antenna, while the width (W_p) of rectangular patch affects the impedance matching. It is found that increasing the L_p parameter shifts the resonant frequency to the lower frequency. As the result, the W_p and L_p parameters are optimized to be 74 mm and 46 mm, respectively. In addition, the size of ground plane is also considered. It is found from simulation results that the size of ground plane does not influence the resonant frequency, but it impacts impedance matching and gain. Increasing the size of ground plane can improve the antenna gain. Therefore, the antenna designer should compromise between antenna size and gain. The width and length of ground plane are optimized to be $W = 82$ mm and $L = 74$ mm, respectively. The conventional rectangular microstrip patch antenna is called Ant. 1. In the second stage of the prototype, the four corners of the rectangular patch with dimensions of $W_1 \times L_1$ and $W_2 \times L_2$ are cut to activate the 5.8 GHz band. Since current and electric field distributions of the conventional microstrip patch antenna are maximum at the edges of radiating patch, cutting four corners can achieve dual resonant frequencies with similar radiating characteristics. It is found from simulated results that when W_1 is

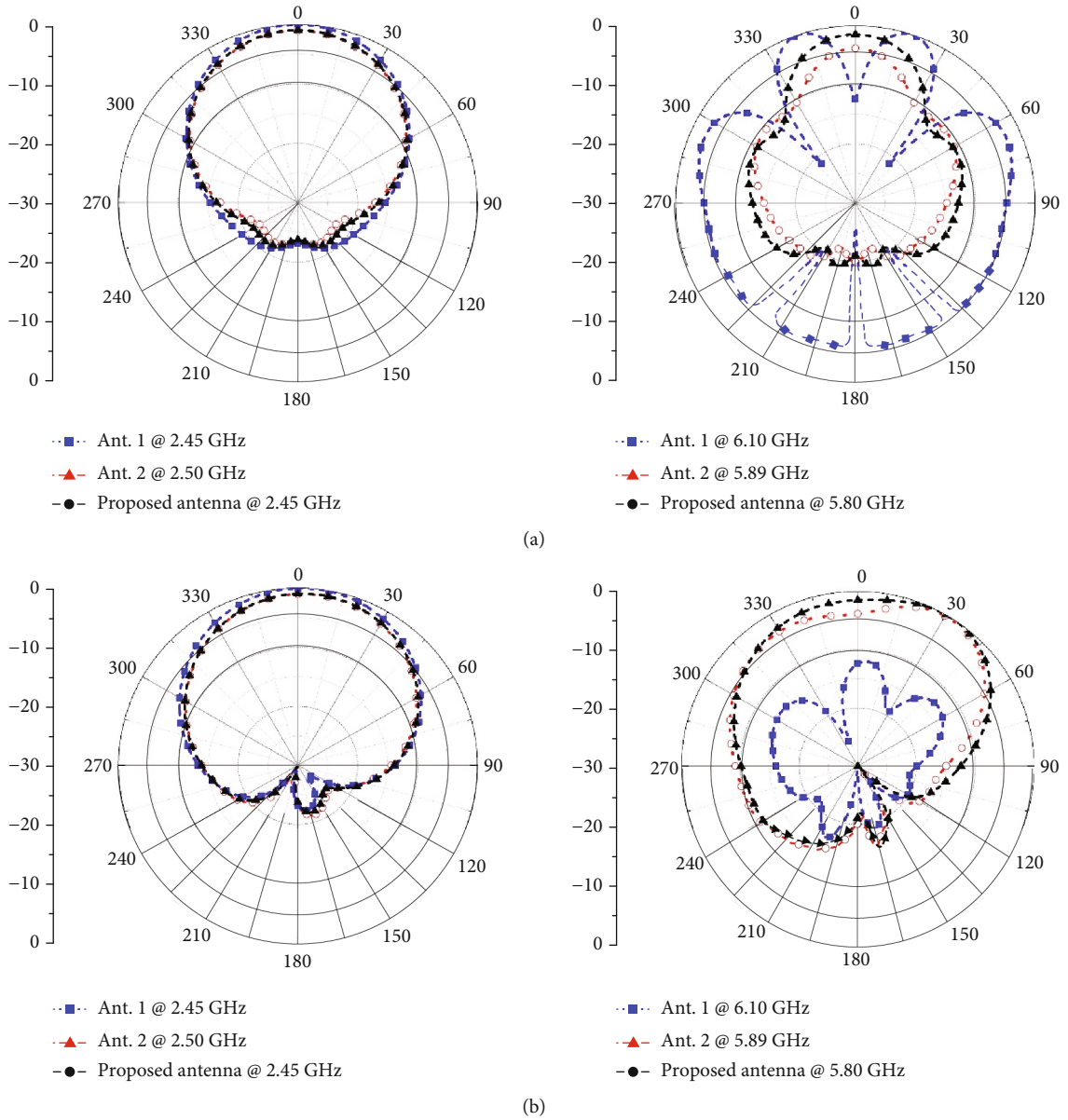

FIGURE 3: The simulated radiation patterns for three antenna design stages: (a) *xz*-plane and (b) *yz*-plane.

increased, the 2.45 GHz band and 5.8 GHz band are shifted to the lower frequency. In addition, when L_1 is increased, the 2.45 GHz band is moved to the lower frequency, whereas the 5.8 GHz band is moved to the higher frequency. For bottom corners' cut, when W_2 is increased, the 2.45 GHz band is shifted to the higher frequency, but on the other hand, the 5.8 GHz band is moved to the lower frequency. Moreover, the increase in L_2 parameter moves the 5.8 GHz band to the higher frequency, but there is no impact on the 2.45 GHz band. The width and length of radiating patch are optimized to be $W_{p1} = 74$ mm and $L_{p1} = 43$ mm, respectively. The microstrip patch antenna with four corners' cut is referred to as Ant. 2. In the third stage, the circular slot is added on the radiating patch to control the designed frequency bands. It is found that the dimension and position of circular slot impact the operating frequencies. When radius (R) of circular slot is increased, the desired operating frequencies in both bands are shifted to the lower frequency. When circular slot is moved away from microstrip feed line, the 5.8 GHz band is shifted to higher frequency, but the 2.45 GHz band remains the same. After optimizing the size and position of the circular slot, the antenna can operate in both of 2.45 GHz and 5.8 GHz bands without radiation distortion. The overall size of proposed antenna is $82 \times 74\,\text{mm}^2$. All antenna parameters and dimensions are summarized in Table 1.

3. Results and Discussion

The proposed antenna was designed and simulated by using the CST microwave studio software. The comparison of the simulated reflection coefficient (S_{11}) of three antenna stages is depicted in Figure 2. It can be observed that the

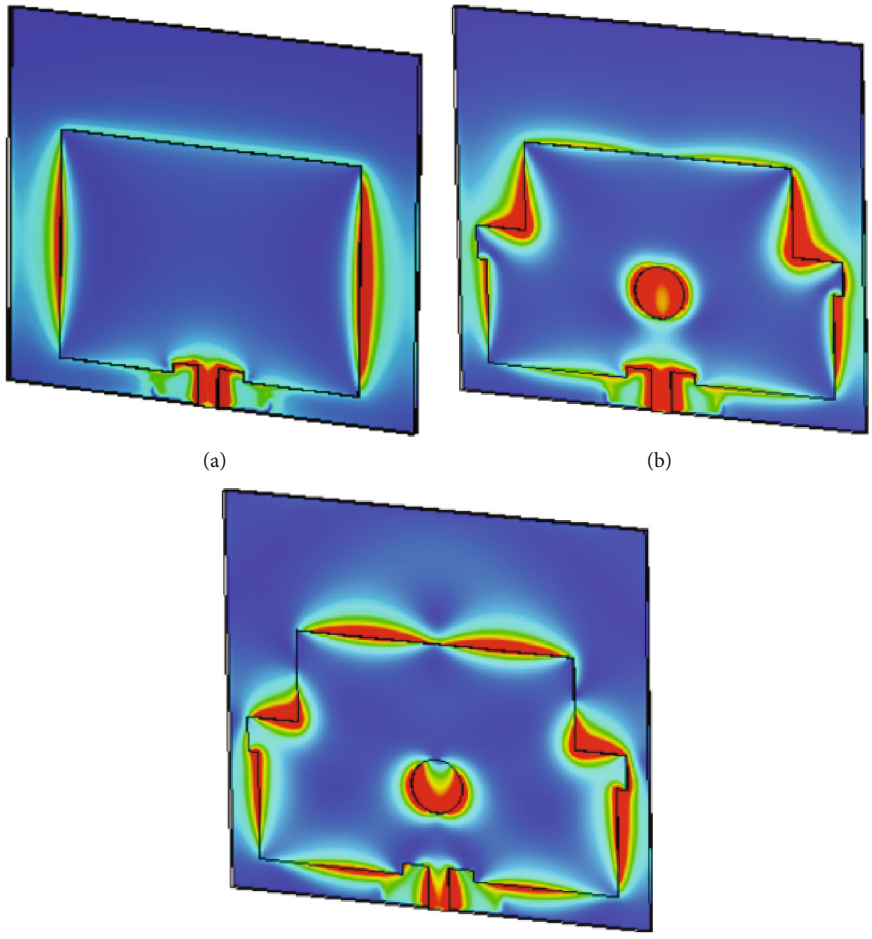

FIGURE 4: Surface current distributions: (a) conventional microstrip patch antenna at 2.45 GHz, (b) proposed antenna at 2.45 GHz, and (c) proposed antenna at 5.8 GHz.

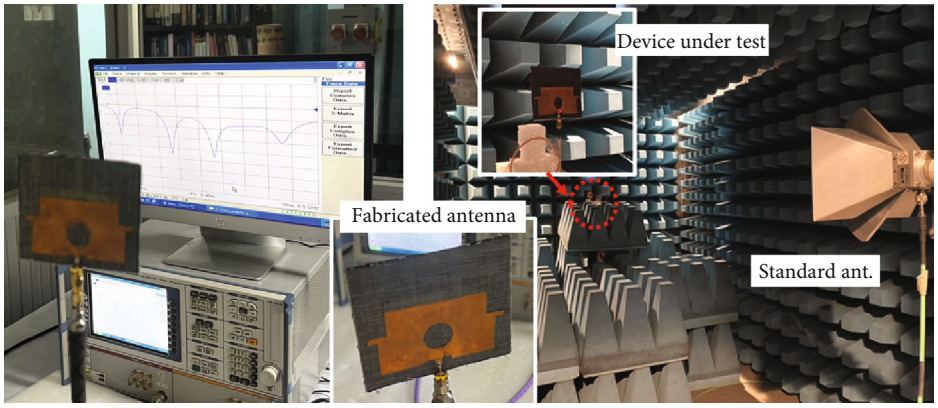

FIGURE 5: Fabricated prototype antenna and experiment setup.

fundamental resonant frequency of the conventional rectangular patch antenna (Ant. 1) is 2.45 GHz with a good impedance matching. Moreover, there are three additional resonant frequencies at 3.06 GHz, 4.01 GHz, and 6.10 GHz, respectively. However, the radiation pattern of the conventional microstrip patch antenna (Ant. 1) has a weak radiation pattern in broadside direction at the higher resonant frequencies as shown in Figure 3. The significant depression in the main radiations at higher frequencies is mainly caused by the destruction of current paths on the left and right

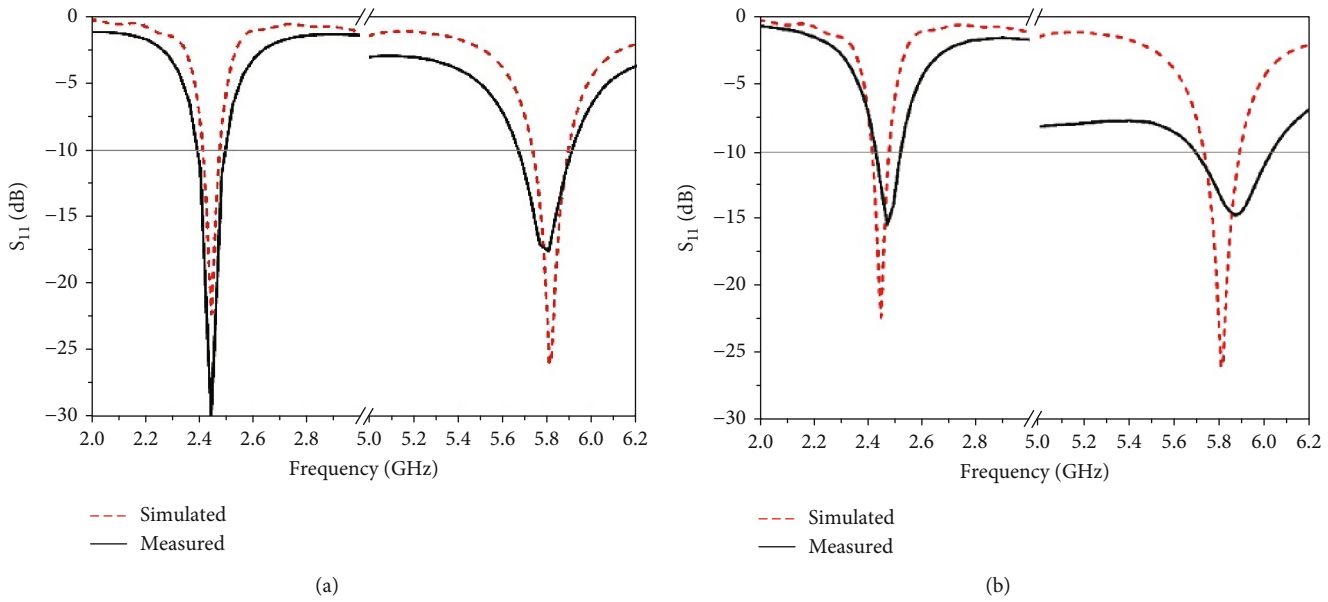

FIGURE 6: The simulated and measured S_{11} of the proposed antenna (a) before bending and (b) after bending.

horizontal components of the rectangular patch. Therefore, the four corners of the rectangular patch are cut with different sizes on the top and bottom corners of the radiating patch. Cutting the four corners of the patch can activate the frequency of 5.89 GHz and can change in the direction of current paths, resulting in the broadside radiation at a 5.8 GHz band. However, the fundamental frequency at 2.45 GHz is shifted toward a higher frequency because the size of the radiating patch is decreased. Thus, the circular slot is etched on the radiating patch to adjust the desired operating frequencies. In this way, the fundamental frequency is moved to 2.45 GHz, and the third resonant frequency is moved to 5.8 GHz. Therefore, etching the circular slot on the radiating patch with the appropriate size and position can help to control the desired operating frequencies. Moreover, adding the circular slot can also enhance the gain at a 0-degree angle (along z-axis) at a 5.8 GHz band. To understand the components of the antenna which play an important role in generating the required operating frequency, the surface current distribution of the conventional microstrip patch antenna and proposed antenna is simulated as shown in Figure 4. The red level shows the contribution portion which influences the operating frequency. It is clearly seen that the current distributions of the proposed antenna at 2.4 GHz are concentrated along the both side edges of radiating patch, microstrip line, and circular slot.

This concentration area is more distributed compared to the conventional microstrip patch antenna. For the current distribution at a frequency of 5.8 GHz, the microstrip line, the radiating edge of patch, and the circular slot are the portions in making the antenna resonate at 5.8 GHz. To confirm the simulated results, the proposed antenna was fabricated and tested as shown in Figure 5. The comparison of simulated and measured reflection coefficient (S_{11}) of the proposed antenna before and after multiple bending is depicted in Figure 6. The measured S_{11} of the proposed antenna before bending shows that the proposed antenna can operate within the desired frequency bands of 2.45 GHz (2.40 GHz–2.49 GHz) and 5.8 GHz (5.67 GHz–5.89 GHz) bands which is in good agreement with the simulated result as shown in Figure 6(a). As explained in antenna design, the dimension of four corners' cut and circular slot impacts the variation of resonant frequency. Therefore, the main differences between simulated and measured S_{11} are possibly related to fabrication error and tolerances of materials used. Then, the antenna is tested in multiple bending operations, which will be discussed in the next section. After bending operations, the proposed antenna still operates within 2.45 GHz and 5.8 GHz bands as shown in Figure 6(b), and the snapshot of the S_{11} measurement on vector network analyzer (VNA) is shown in Figure 5. However, the impedance matching is worse due to partial deformation of the patch and ground plane.

The radiation pattern and gain of the proposed antenna are measured in an anechoic chamber. The simulated and measured radiation patterns in the xz-plane and yz-plane at 2.45 GHz and 5.8 GHz are shown in Figure 7. The results show that the radiation patterns of the proposed antenna are unidirectional at both operating frequencies of 2.45 GHz and 5.8 GHz. The proposed antenna shows good broadside radiations at desired resonant frequencies. It is known that the textile-based antennas with broadside radiation patterns are commonly required for linking with external devices, since in wearable applications, only the energy forward direction can be utilized while the backward direction is absorbed by human body. Therefore, the designed antenna is useful for a body-to-external device link of WBAN applications. In addition, it is safe when used on human body. The maximum realized gains of the proposed antenna at 2.45 GHz and 5.8 GHz are 4.22 dBi and 3.22 dBi in the simulation and 3.08 dBi and 2.15 dBi in the measurement. The difference between simulated and measured results of radiation patterns and gains is possibly caused by misalignment

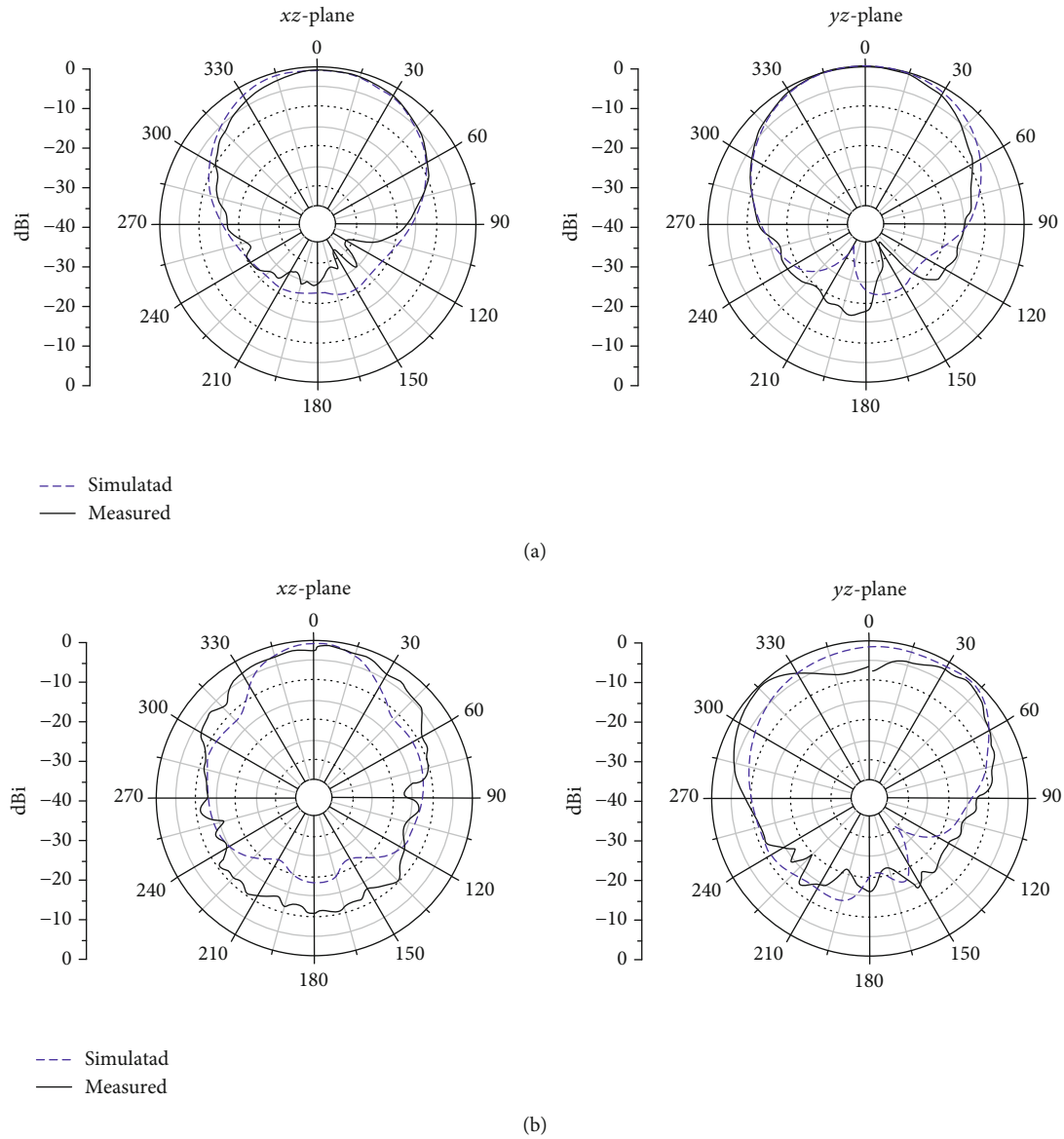

Figure 7: The simulated and measured radiation patterns in the *xz*-plane and *yz*-plane: (a) 2.45 GHz and (b) 5.8 GHz.

between transmitting and receiving antennas, tolerance of fabrication, tolerances of materials used, and the loss from adhesive layer.

In practical applications, the wearable or flexible antennas must be bent during operation. Therefore, the effects of bending on antenna characteristics are investigated. The antenna is bent around the *x*-axis (in the *L* direction) and *y*-axis (in the *W* direction), corresponding to cylindrical radius along *x*-axis (R_x) and *y*-axis (R_y). Four bending radii along each axis, namely, 30, 40, 50, and 60, are studied. The selected radii are based on the typical size of human arms and legs. The simulated S_{11} of the proposed textile antenna without bending (flat) and with different bending radii around *x*-axis is depicted in Figure 8. In the case without bending, the impedance bandwidth of antenna in free space is 2.45% (2.42-2.48 GHz) and 2.75% (5.73-5.89 GHz), covering the ISM band. When the bending radius R_x is decreased from 70 to 30 mm (bending degree increases), the operating frequencies at 2.45 GHz and 5.8 GHz are significantly shifted to lower frequency. The proposed antenna cannot operate within the 2.45 GHz band when bending radius is less than 40 mm. At the 5.8 GHz band, the antenna cannot operate in this bending condition. It is because the surface current is mainly along *y*-axis (in the *L* direction); therefore, bending in this direction strongly impacts the operating frequency. The proposed antenna may not be suitable for mounting on curved surface along its length. Meanwhile, bending the antenna around *y*-axis (in the *W* direction), the frequency band of 2.45 GHz is also shifted to lower frequency, and impedance matching is poor as the bending radius R_y decreases from 70 to 30 mm as shown in Figure 9. In addition, the frequency band of 5.8 GHz is also shifted to a lower frequency as the radius decreases. However, the proposed antenna still operates at 2.45 GHz and 5.8 GHz bands under

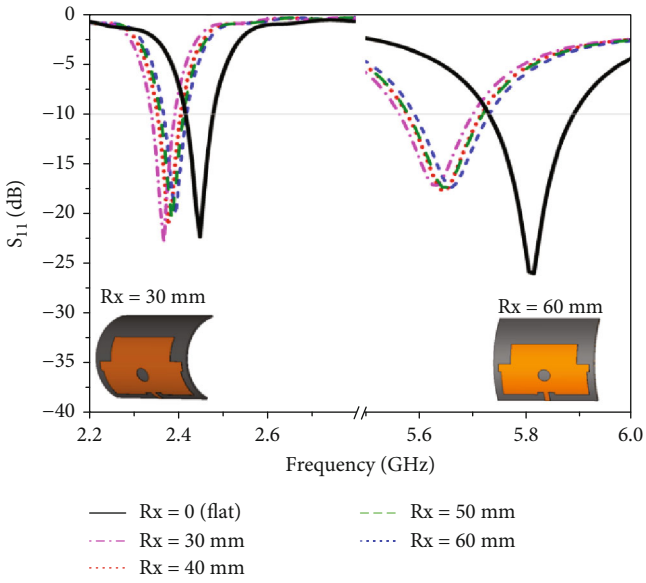

FIGURE 8: The simulated S_{11} with different bending radii around x-axis.

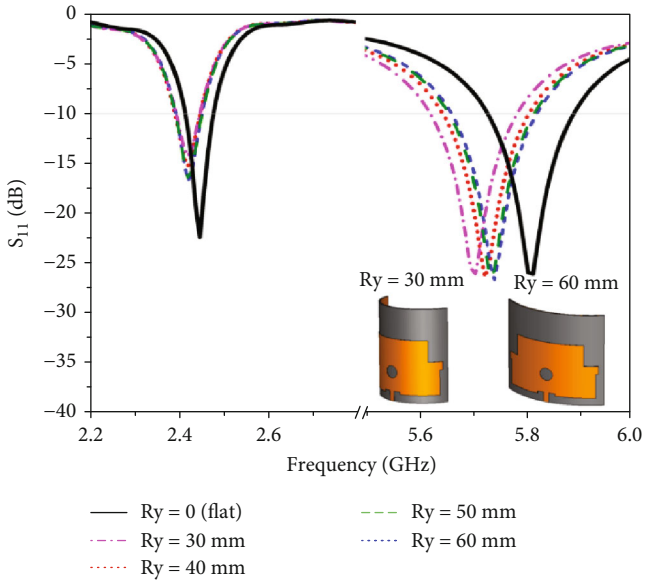

FIGURE 9: The simulated S_{11} with different bending radii around y-axis.

this bending condition. To confirm the simulated results, the prototype antenna was placed on the curved surface of cylindrical foam with a radius (R) of 30 mm and 50 mm. The measured S_{11} of prototype antenna bent on cylindrical foam is illustrated in Figure 10. It can be observed that the measured S_{11} of the prototype antenna on cylindrical foam show a similar trend with simulation, but it provides a wider bandwidth in both 2.45 and 5.8 bands. The proposed antenna still serves the WBAN application at 2.45 and 5.8 GHz bands.

To investigate the impact of the human body on antenna performance, the antenna is positioned on two different

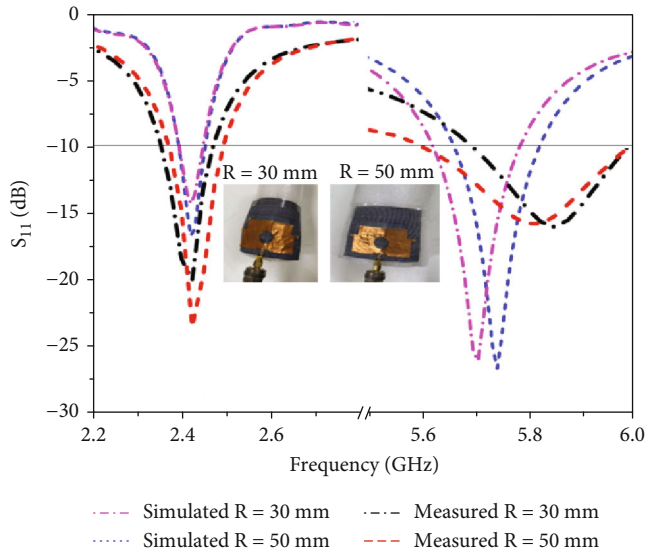

FIGURE 10: The simulated and measured S_{11} of antenna for chosen bending radii.

areas of the human body: the belly (flat surface) and the arm (curved surface), as illustrated in Figure 11. To replicate the shape of the belly, the model is defined as a square measuring 150 mm × 40 mm. To mimic the shape of the arm, a cylinder with a radius of 40 mm and a length of 150 mm is designed. Both models comprise four layers: skin, fat, muscle, and bone, with the tissue parameters for each layer summarized in Table 2 [7]. The proposed antenna is placed on each of the model in the simulation. The S_{11} values of the proposed antenna when placed on the belly and in free space are compared, as shown in Figure 12. In the simulation, there is no gap between antenna and belly model. However, in the measurement, there may be a small gap between antenna and human belly. It is found that the measured S_{11} values in both the free space and on the belly exhibit a consistent trend with the simulated results. Observing the measured S_{11} values, it becomes evident that the impedance matching of the prototype antenna, when placed on the belly, deteriorates compared to when the antenna is in free space. Moreover, the measured S_{11} of antenna on the belly shows a slight shift toward higher frequencies compared to antenna in free space. The reason for frequency shift is because the human body acts as an additional lossy substrate layer which has different dielectric constant. Therefore, the presence of lossy dielectric on the antenna causes significant changes to its input impedance [28]. This introduces an impedance mismatch and causes a shift in the operating frequency of the antenna. It is found from simulated results that the gap between antenna and skin slightly affects the S_{11} but significantly affects the specific absorption rate (SAR) by human body. As antenna is far away from the human body, the SAR value will decrease. In case the antenna is bent and placed on the arm, the antenna is mounted on a foam sheet with a thickness of 3 mm as depicted in Figure 11(b). Figure 13 displays the simulated and measured S_{11} values for the proposed antenna, both when positioned on the arm and in free space. The measured

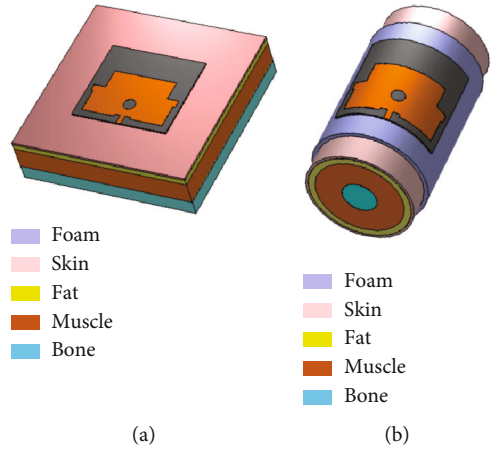

FIGURE 11: The proposed antenna is on the (a) belly model and the (b) arm model.

TABLE 2: Parameters of the human tissue model.

Tissue types	ε_r	σ (S/m)	Density (kg/m^3)	Thickness (mm)
Skin	37.95	1.49	1001	2
Fat	5.27	0.11	900	5
Muscle	52.67	1.77	1006	20
Bone	18.49	0.82	1008	13

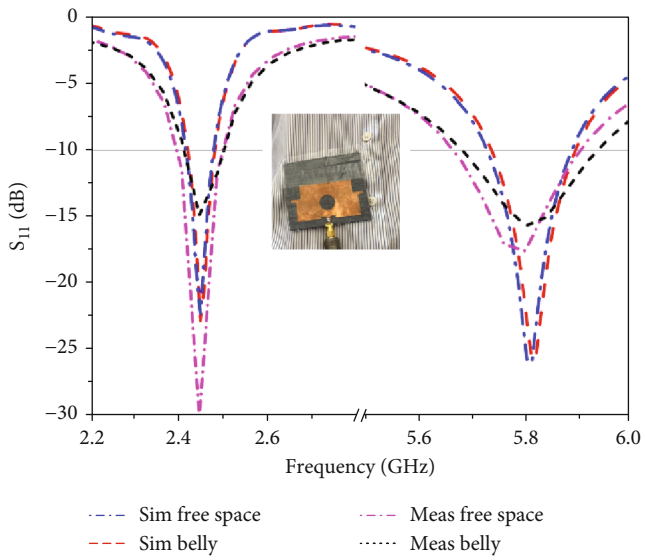

FIGURE 12: The simulated and measured S_{11} of the proposed antenna on belly and in free space.

results show a similar trend compared to the simulation. It is known that bending and human body strongly influence on the antenna performance, especially the operating frequency. Thus, the desired operating frequencies are shifted to the upper frequency when antenna is placed on the arm. However, by bending the proposed antenna and placing it on the arm, it still operates within the 2.45 GHz and 5.8 GHz ISM bands. Furthermore, the simulated 3D patterns

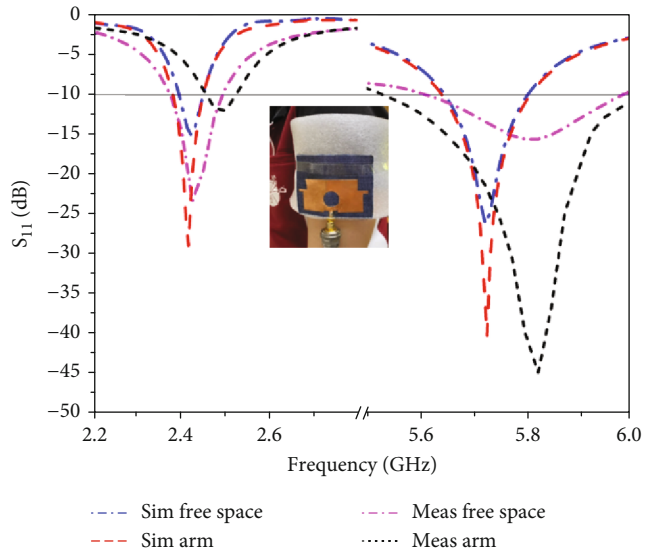

FIGURE 13: The simulated and measured S_{11} of the proposed antenna on arm and in free space.

of the proposed antenna on belly and arm at 2.45 GHz and 5.8 GHz are depicted in Figure 14. The radiation patterns of the proposed antenna placed on belly models are slightly changed compared with the radiation pattern in free space. Placing the antenna on arm model results in decreasing the gain as well as increasing the back lobe and beamwidth. However, the radiation patterns of proposed antenna on human body still maintain in the broadside direction (z-axis).

To evaluate the effects of the proposed antenna on the human body, the specific absorption rate (SAR) is simulated. The SAR is known as the rate of RF energy absorbed by human body per unit tissue mass, and its unit is W/kg [29]. According to the FCC standard, the SAR value should not exceed 1.6 W/kg averaged over 1 g of tissue. The SAR value was calculated by CST studio software. The input power for calculation is set as 0.5 W. The SAR value on belly and arm models is illustrated in Figure 15. According to the SAR value on the color bar, the red region indicates a high energy density of the antenna radiation on the human tissue model. For the belly model, the maximum SAR values calculated according to the FCC standard are 0.258 W/kg at 2.45 GHz and 0.185 W/kg at 5.8 GHz as depicted in Figure 15(a), which are far below the FCC limit. For the arm model, we found from the simulated results that the SAR value, when antenna is placed directly on the arm, is 2.307 W/Kg at 2.45 GHz and 0.781 W/kg at 5.8 GHz. The SAR value at 2.45 GHz exceeds the FCC limit. Therefore, the antenna is placed on foam with the thickness of 3 mm to prevent the antenna from touching the arm. As seen in Figure 15(b), the SAR values on the arm decrease to be 0.1046 W/kg at 2.45 GHz and 0.1121 W/kg at 5.8 GHz, which obey the FCC standard.

The comparison between the proposed textile microstrip patch antenna and other textile microstrip patch antennas reported in the literature is shown in Table 3. It is well known that the radiation pattern of microstrip patch antenna with full ground plane is perpendicular to antenna

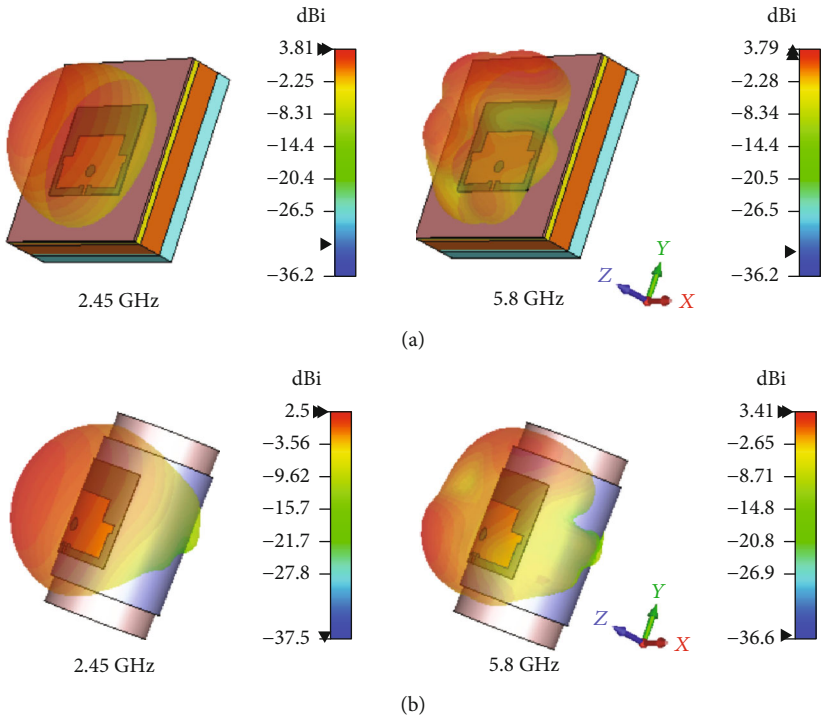

Figure 14: The 3D radiation patterns of the proposed antenna on (a) belly and (b) arm.

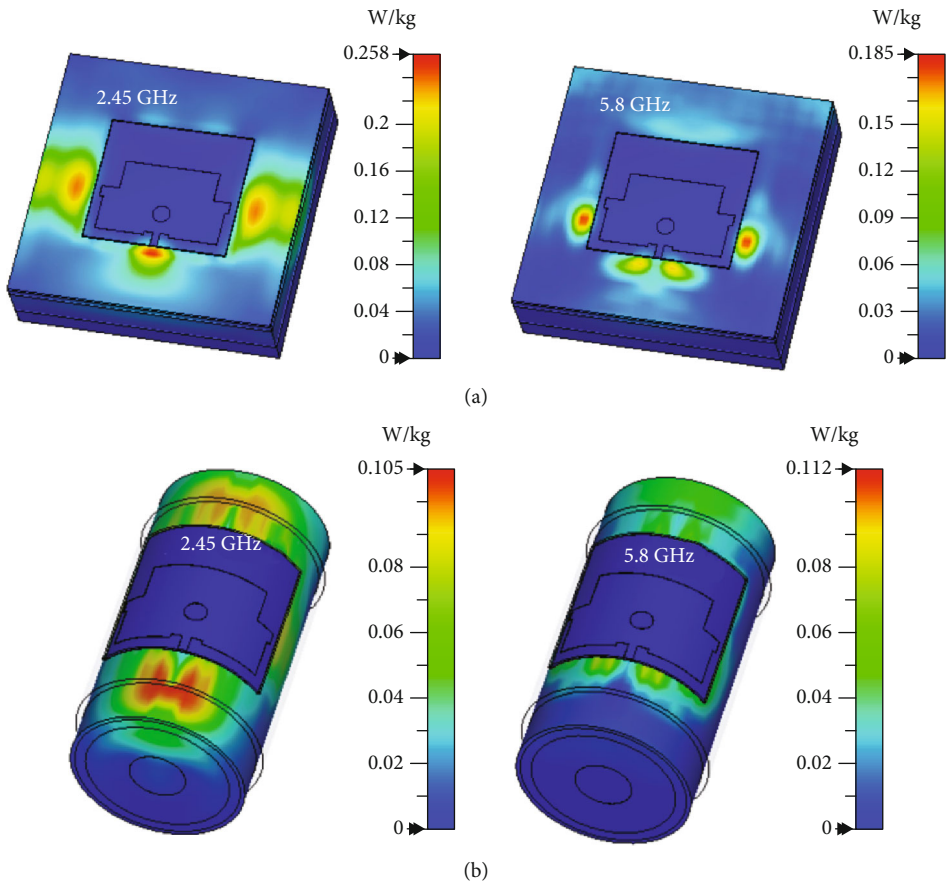

Figure 15: The SAR values evaluated over 1 g of tissue of the proposed antenna at 2.45 GHz and 5.8 GHz on the (a) belly model and the (b) arm model.

Table 3: Comparison between the proposed antenna and other flexible microstrip patch antenna in literature.

Ref. no	Frequency (GHz)	Overall size (mm^3)	Substrate material	Gain (dBi)	SAR (W/kg)
[22]	2.45/3.3/5.8	$60 \times 60 \times 1.17$	Denim	-0.94/-2.65/3.09	0.11/0.33
[23]	2.4/5.8	$64.36 \times 76.96 \times 4.06$	Fleece/felt	5.7/6.8	12.33/8.037
[24]	2.53/4.9/7.6	53.2×58.7	Jean	8.61/3.92/5.38	—
[25]	2.45/3.9/6.56	$50 \times 80 \times 0.56$	Jean	4.71/-/-	—
Proposed	2.45/5.8	$74 \times 82 \times 1$	Jean	3.08/2.15	0.258/0.185

plane. Therefore, when antenna is mounted on the body, the amount of back lobe that radiates toward the body is low and safe for the human body. In [22], the triple-band antenna was designed having compact size, but the gain is very low at a low frequency in comparison with the proposed antenna. The antenna in [23] can operate two frequency bands, but the SAR value is very high beyond the FCC limit. The research work in [24] is based on microstrip patch antenna and hybrid fractal antenna. Although this antenna provides compact size and high gain, the main lobe of the pattern is tilted, and the back lobe increases at high frequency. Moreover, using the DGS on the ground plane causes the back lobe and SAR value to exceed standard. In [25], the antenna covers multifrequency bands by cutting the rectangular on the ground plane to obtain a designed resonant frequency. The antenna has a bidirectional radiation pattern which can yield the SAR value exceeding the standard. Compared to related works, the proposed dual-band textile microstrip patch antenna achieves a simpler structure, low profile, low complexity in design, low cost, and low SAR while providing acceptable gain and stable radiation pattern in both bands. Therefore, the proposed antenna is a good candidate for wearable, IoT, and WBAN applications.

4. Conclusions

Low-profile, dual-band textile microstrip patch antenna operating at 2.45 GHz and 5.8 GHz ISM bands for WBAN application was presented. The proposed antenna consists of a simple rectangular patch and full ground plane. The novelty of the proposed antenna is cutting the four corners of radiating patch and adding the circular slot into the patch to excite a new resonant frequency while the radiation characteristics of fundamental resonant frequency are kept unaltered. By using these techniques, the proposed antenna achieves dual-band characteristics with stable broadside radiation patterns and low SAR in both two bands without complexity in design. The proposed antenna provides simple and low-profile structure, compact size, flexibility, safety, and comfort in wearing. The simulated and measured results can confirm that the proposed antennas are suitable for a wide variety of WBAN applications.

Data Availability

The data used to support the findings of this study are included within the article.

Conflicts of Interest

The authors declare that there are no conflicts of interest. There is no conflict of interest with the coauthors.

Acknowledgments

This research was funded by the National Science, Research and Innovation Fund (NSRF) and the King Mongkut's University of Technology North Bangkok with Contract no. KMUTNB-FF-66-47. Moreover, the authors gratefully acknowledge the Department of Electrical and Computer Engineering, Faculty of Engineering, King Mongkut's University of Technology North Bangkok for equipment and support for this research work.

References

[1] R. Negra, I. Jemili, and A. Belghith, "Wireless body area networks: applications and technologies," *Procedia Computer Science*, vol. 83, pp. 1274–1281, 2016.

[2] U. Ali, S. Ullah, B. Kamal, L. Matekovits, and A. Altaf, "Design, analysis and applications of wearable antennas: a review," *IEEE Access*, vol. 11, pp. 14458–14486, 2023.

[3] M. A. S. M. AL-Haddad, N. Jamel, and A. N. Nordin, "Flexible antenna: a review of design, materials, fabrication, and applications," *Journal of Physics: Conference Series*, vol. 1878, no. 1, article 012068, 2021.

[4] H. M. Madjar, "Human radio frequency exposure limits: an update of reference levels in Europe, USA, Canada, China, Japan and Korea," in *2016 International Symposium on Electromagnetic Compatibility - EMC EUROPE*, pp. 467–473, Wroclaw, Poland, September 2016.

[5] E. Li, X. J. Li, and B.-C. Seet, "A low-profile wideband monopole antenna for WBAN flexible applications," in *2022 IEEE 9th International Symposium on Microwave, Antenna, Propagation and EMC Technologies for Wireless Communications (MAPE)*, pp. 101–104, Chengdu, China, August 2022.

[6] S. Morris, A. R. Chandran, N. Timmons, and J. Morrison, "Design and performance of a flexible and conformai PDMS dipole antenna for WBAN applications," in *2016 46th European Microwave Conference (EuMC)*, pp. 84–87, London, UK, October 2016.

[7] G.-P. Gao, B. Hu, S.-F. Wang, and C. Yang, "Wearable circular ring slot antenna with EBG structure for wireless body area network," *IEEE Antennas and Wireless Propagation Letters*, vol. 17, no. 3, pp. 434–437, 2018.

[8] A. Arif, M. Zubair, M. Ali, M. U. Khan, and M. Q. Mehmood, "A compact, low-profile fractal antenna for wearable on-body

WBAN applications," *IEEE Antennas and Wireless Propagation Letters*, vol. 18, no. 5, pp. 981–985, 2019.

[9] N. Sakib, S. N. Ibrahim, M. I. Ibrahimy, M. S. Islam, and M. M. H. Mahfuz, "Design of microstrip patch antenna on rubber substrate with DGS for WBAN applications," in *2020 IEEE Region 10 Symposium (TENSYMP)*, pp. 1050–1053, Dhaka, Bangladesh, June 2020.

[10] Z. Yu, G. Zhang, X. Ran et al., "A flexible multiband dendritic structure fractal antenna for 4G/5G/WLAN/Bluetooth applications," *International Journal of RF and Microwave Computer-Aided Engineering*, vol. 2023, Article ID 6496757, 8 pages, 2023.

[11] M. Aprizal, L. O. Nur, B. S. Nugroh, and A. Munir, "Flexible artificial magnetic conductor reflector for wearable antenna application," in *Progress in Electromagnetics Research Symposium (PIERS-Toyama)*, pp. 1859–1862, Toyama, Japan, August 2018.

[12] B. Kumkhet, P. Rakluea, N. Wongsin et al., "SAR reduction using dual band EBG method based on MIMO wearable antenna for WBAN applications," *International Journal of Electronics and Communications*, vol. 160, article 154525, 2023.

[13] B. Sugumaran, R. Balasubramanian, and S. K. Palaniswamy, "Performance evaluation of compact FSS-integrated flexible monopole antenna for body area communication applications," *International Journal of Communication Systems*, vol. 35, no. 6, 2022.

[14] T. H. Dam, M. T. Le, Q. C. Nguyen, and T. T. Nguyen, "Dual-band metamaterial-based EBG antenna for wearable wireless devices," *International Journal of RF and Microwave Computer-Aided Engineering*, vol. 2023, Article ID 2232674, 11 pages, 2023.

[15] S. Panda, A. Gupta, and B. Acharya, "Wearable microstrip patch antennas with different flexible substrates for health monitoring system," *Materials Today: Proceedings*, vol. 45, Part 4, pp. 4002–4007, 2021.

[16] R. Salvado, C. Loss, R. Gonçalves, and P. Pinho, "Textile materials for the design of wearable antennas: a survey," *Sensors*, vol. 12, no. 11, pp. 15841–15857, 2012.

[17] C. Ahumada, H. Kaschel, and R. Osorio-Comparan, "Design of wearable textile patch antenna at 2.45 GHz for WBAN applications," in *2021 IEEE CHILEAN Conference on Electrical, Electronics Engineering, Information and Communication Technologies (CHILECON)*, pp. 1–5, Valparaíso, Chile, December 2021.

[18] C. C. Clara, S. S. Rebecca, J. S. Ashick, and N. Moses, "Design and development of microstrip patch antenna for tumor detection," in *2023 International Conference on Innovative Data Communication Technologies and Application (ICIDCA)*, pp. 1021–1028, Uttarakhand, India, March 2023.

[19] E. Li, X. J. Li, and B.-C. Seet, "A triband slot patch antenna for conformal and wearable applications," *Electronics*, vol. 10, no. 24, p. 3155, 2021.

[20] U. Musa, S. M. Shah, H. A. Majid et al., "Design and analysis of a compact dual-band wearable antenna for WBAN applications," *IEEE Access*, vol. 11, pp. 30996–31009, 2023.

[21] L. Zhou, S. J. Fang, and X. Jia, "A compact dual-band and dual-polarized antenna integrated into textile for WBAN dual-mode applications," *Progress In Electromagnetics Research Letters*, vol. 91, pp. 153–161, 2020.

[22] H. Li, J. Du, X.-X. Yang, and S. Gao, "Low-profile all-textile multiband microstrip circular patch antenna for WBAN applications," *IEEE Antennas and Wireless Propagation Letters*, vol. 21, no. 4, pp. 779–783, 2022.

[23] K. A. Malar and R. S. Ganesh, "Novel aperture coupled fractal antenna for internet of wearable things (IoWT)," *Measurement: Sensors*, vol. 24, article 100533, 2022.

[24] S. S. Sran and J. S. Sivia, "ANN and IFS based wearable hybrid fractal antenna with DGS for S, C and X band application," *International Journal of Electronics and Communications*, vol. 127, article 153425, 2020.

[25] H. Kaur and P. Chawla, "Performance analysis of novel wearable textile antenna design for medical and wireless applications," *Wireless Personal Communications*, vol. 124, no. 2, pp. 1475–1491, 2022.

[26] Y. Hengroemyat, T. Kaewthai, P. Akkaraekthalin, and W. Thaiwirot, "A flexible dual-band antenna with stable radiation pattern for wearable application," in *2023 20th International Conference on Electrical Engineering/Electronics, Computer, Telecommunications and Information Technology (ECTI-CON)*, pp. 1–4, Nakhon Phanom, Thailand, May 2023.

[27] C. A. Balanis, *Antenna Theory: Analysis and Design*, John Wiley & Sons, Inc., Hoboken, New Jersey, 2016.

[28] S. A. Balakrishnan and E. F. Sundarsingh, "Conformal self-balanced EBG integrated printed folded dipole antenna for wireless body area networks," *IET Microwaves, Antenna & Propagation*, vol. 13, no. 14, pp. 2480–2485, 2019.

[29] A. A. R. Saad, W. M. Hassan, and A. A. Ibrahim, "A monopole antenna with cotton fabric material for wearable applications," *Scientific Reports*, vol. 13, no. 1, p. 7315, 2023.